Novel concepts for noise mitigation of small UAV rotors

Pedro Miguel de Barros e Silva Duarte
pedro.s.duarte@tecnico.ulisboa.pt

Instituto Superior Técnico, Universidade de Lisboa, Portugal

October 2020

Abstract

The objective was to study the noise produced by a small UAV rotor in hover conditions and achieve noise reductions by implementing leading edge and trailing edge modifications. Using additive manufacturing, three leading edge modified rotors and three trailing edge serrated rotors were constructed and then experimentally tested against a baseline. The tests were conducted in the anechoic chamber of the Aeroacoustic Tunnel of Instituto Superior Técnico.

The trailing edge serrations were confirmed to reduce consistently the high frequency noise. Considering the overall noise, the reductions achieved depended on the operating rotation speed. However, this type of serrations showed to degrade the aerodynamic performance of the rotors, generating less thrust and requiring more power than the baseline.

The sinusoidal leading edges implemented proved to be effective in reducing the noise for the frequencies to which the human hearing is most sensitive to. Furthermore, they also showed small reductions in the high frequency noise, although not as much as the trailing edge serrations. These rotors presented either small losses to the aerodynamic performance or, in the case of one of the rotors, an increase in the generated thrust and in the figure of merit.

Keywords: Rotor noise; Blade serrations; Trailing edge serrations; Leading edge modifications.

1. Introduction

Noise pollution is a major topic currently being approached. Any noise source can directly disturb the health quality of those around it. Noise is produced by machines, engines and all kinds of devices, and all of these are products of engineering. As such, it is possible to study it and, therefore, improve the technology employed in order to minimize noise emissions.

The present study focuses on the noise emissions of a small UAV rotor, how to reduce it and at what costs to the aerodynamic performance.

2. Topic Overview - The Aerodynamic Noise

The aerodynamic noise generated by an aerofoil is divided into two types: the turbulent inflow noise and the aerofoil self-noise.

The turbulent inflow noise occurs during the interaction between the blade's Leading Edge (LE) with the upstream atmospheric turbulence. In a simplistic way, this noise will be greater the greater the size of the eddies, in the incoming flow, interacting with the blade's LE. Therefore, this noise will depend on the atmospheric conditions and on the flow velocity.

The aerofoil self-noise is the noise inherent to the blade itself, hypothetically considering that the blade is rotating in an undisturbed flow. This noise divides into different contributions, the most important ones being the blade tip vortex noise and the Trailing Edge (TE) noise. The first one, as the name suggests, is related with the vortex created at the blade tip, which in turn is affected by the blade tip speed. The TE noise is related with the development of the boundary layer over the aerofoil. Summarizing, this noise will be louder when the turbulent boundary layer thickness nearing the TE is higher. As such, the vortical structures trailing from the TE will create more powerful noise sources across the TE.

The aerodynamic noise has been studied for some decades now, at least dating back to the seventies with Amiet [1, 2], when he developed analytical methods for calculating the far field noise produced by an aerofoil in a subsonic turbulent stream. Amiet even extended his studies by reaching a theoretical method to calculate the TE noise from an aerofoil in an incident turbulent flow. Later, in the late eighties and early nineties, Howe [3, 4] analysed analytically the diffraction problem on a flat plate with a serrated TE. Howe also predicted, numerically, the noise reduction levels for different TE serrations and analysed different wavelength-to-amplitude serration ratios, concluding that the

optimal attenuation should be obtained with the sawtooth type of serration. Recently, other analytical and numerical studies have been performed, for both LE and TE modifications, as the ones by Sinayoko, Azarpeyvand and Lyu [5, 6].

2.1. Trailing Edge Serrations

In general, the TE modifications tested are usually serrations, that is cuts into the wing or blade itself to assimilate a desired shape, for example as a sawtooth or a sinusoidal TE. Concerning serrations, it is generally considered that the serration is periodic, having a wavelength λ and an amplitude $2h$, as it is shown in Figure 1, and most of these studies perform a parametric analysis around those two variables.
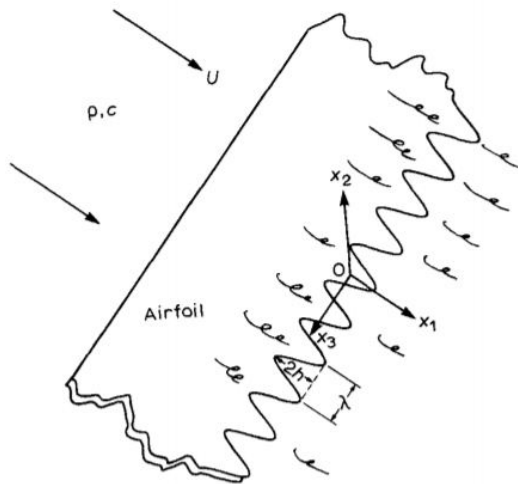

Figure 1: Aerofoil with serrated TE. Figure taken from [3].

Gruber [7] tested 30 different serrated TEs on a wing, comparing with Howe's predictions for the noise reductions of a sawtooth TE configuration, and concluded several important notions. The first one states that the noise frequency f up to which there is noise reduction is determined by the Strouhal number $St_\delta = f.\delta/U_0$ based on the boundary layer thickness δ, where U_0 is the upstream flow velocity. For Strouhal numbers $f.\delta/U_0 > 1$ there is a noise increase for the given frequencies, whereas for $f.\delta/U_0 < 1$ the noise is reduced and the level of its reduction depends on the ratios h/δ and h/λ. The second notion is that for $h/\delta < 0.5$, the noise reduction attained is insignificant across the entire frequency range. In this case, the serration amplitude h is clearly shorter than the length of the eddies, making these pass over the serrations unperturbed just as if there was no TE serration. Finally, it was concluded that the serration amplitude should be greater than the wavelength and that increasing h/λ would increase the noise reduction.

Concerning rotors, which are the case study of this thesis, there are fewer studies for them than for wings. Lee *et al.* [8] performed an experimental study to assess both the aeroacoustic noise and the aerodynamic performance of relatively small rotors. The Sound Pressure Level (SPL) and the thrust generated were measured for four different rotors: a baseline; a sawtooth serrated TE on half of the blade span; a sawtooth serrated TE on a quarter of the blade span; and a rectangular serrated TE. It was concluded that the effectiveness of the serrations vary with the rotation speed, with the half-span serrated rotor performing better (in terms of noise reduction) at certain speeds while the quarter-span serrated rotor performs better on others. Overall, for these two rotors, as the rotation speed increases, the percentage of thrust lost (compared with the baseline) increases.

2.2. Leading Edge Modifications

Hersh and Hayden [9] addressed the sound radiation from both wings and rotors, affirming that loud tones radiate from these lifting surfaces, generated by vortexes being shed into the aerofoil and propeller wake at a periodic rate. However, with the use of well positioned LE serrated strips it was possible to remove these tones. Soderman also studied the use of serrated strips on the LE, initially the aerodynamic effects caused by them [10], and then the noise reduction effects on low speed rotors [11]. Soderman concluded that the serrations were definitely more effective in reducing the noise at low tip speeds rather than at high tip speeds. Furthermore, the high frequency noise was the one that decreased the most, considering that the noise reductions ranged from 4 to $8dB$ on the Overall Sound Pressure Level (OASPL), with reductions of 3 to $17dB$ in the high octave bands. Later, Hersh, Soderman and Hayden [12] continued the investigation on the use of serrated strips both on wings as on small rotors. They stated that the dominant region of noise generation was the outer one-quarter of the blade radius, finding that the serrations had a clear effect on reducing the broadband noise. This reduction was attributed to a serration vortex generation that mitigated the wake-induced aerofoil noise. Plus, the serrations would also cause a faster dissipation to the tip vortexes, diminishing the tip vortex noise generation.

Considering the modifications to the LE, they do not consist only on serrated strips. There are also serrations on the body itself, but not exactly like the TE serrations, since these are cutouts. In the LE it is important to maintain a smooth and continuous surface, so these serrations preserve the 2D profile and aerodynamic characteristics. For that reason, the most common LE serration is the sinusoidal one, although there are also some studies which

approach sawtooth serrations as well. Chong *et al.* [13] performed a parametric analysis on the serration's amplitude and wavelength, evaluating their influence on the noise generated and also on the aerodynamic characteristics. They reached the following conclusions: First, increasing h benefits the noise reduction, but would decrease the lift coefficient and the lift curve slope. Second, increasing λ delays the stall angles, but the lift coefficient at pre-stall conditions becomes lower compared to the baseline. Third, the largest noise reduction peak occurs with the highest λ and h. However, these values would increase significantly the high frequency noise. Fourth, for the best reduction of the OASPL, large h and small λ are advisable. And finally fifth, to improve the aerodynamic lift, small h and large λ are advisable.

Following Chaitanya's *et al.* research [14], the origin of the turbulent inflow noise becomes more clear, stating that maximum noise reductions can be achieved when the turbulence integral length-scale Λ equals one half of the serration wavelength. Plus, it shows that the noise reductions normally increase with increasing frequency until the frequency where the aerofoil self-noise becomes predominant. Furthermore, it implies that the total noise radiated is dominated by the turbulent inflow noise (generated in the LE) at low frequencies, whereas the TE noise dominates at high frequencies. As such, the effectiveness of LE serrations is limited by the dominance of aerofoil self-noise, which can be approached with the use of TE serrations.

Roger *et al.* [15] studied the turbulence impingement noise reduction with the use of a wavy LE serration (or tubercles, as the authors name them) and a porous serrated TE, on a NACA-0012 aerofoil. They state that a properly shaped serration on the LE has beneficial effects aerodynamically and acoustically, because these serrations prevent the flow from separating and delay the onset of stall.

3. Implementation
3.1. Design of the Blades

Seven different rotors were designed and manufactured, of which 3 contain TE serrations, other 3 have LE serrations, and the last one is the baseline. Each type of serration is implemented in three different blade span percentages: one in only 20% of the blade span; other in 40% of the blade span; and another at 60% of the blade span. Figure 2 presents all the rotors experimentally tested.

For the blades, the NACA-0018 aerofoil was chosen because it is one of the most studied aerofoils and it has a relatively high thickness. Every blade has a radius of $R = 17.78cm$ and a linear varying twist from root to tip of $12°$ to $2°$. The blades were 3D-printed with a Polylactic Acid (PLA) filament.

Figure 2: All tested rotors.

3.1.1 Trailing Edge Serrations

Howe stated that a wavelength-to-amplitude ratio such that $\lambda/h \geq 10$ would result in a noise attenuation of $1dB$, whereas with the ratio $\lambda/h = 1$ resulted in approximately $8dB$ of attenuation. Howe then concluded that to obtain optimal attenuation, one should use sawtooth serrations, as opposed to TE sinusoidal serrations, with the edges formed by the serrations inclined at less than $\theta = 45°$ to the mean flow. So, considering Howe's findings, Lee's experimental study and keeping in mind Gruber's conclusions, the sawtooth serration parameters of the TE serrated blades were defined as the following:

- The amplitude $2h$ varies along the span and equals to 1/4 of the blade chord;

- The wavelength λ is defined by the ratio $\lambda/h = 0.9$, the same followed by Lee;

- The angle θ is automatically defined by the two previous parameters, and it is equal to $13°$;

- The flat tip width a was chosen to be 1/2 of the serration wavelength.

The flat tips increase the effective surface area, therefore helping not to lose some of the lift that is lost with the serrations. This dimension was chosen to vary linearly along the span, just as the amplitude and the wavelength.

3.1.2 Leading Edge Serrations

In the case of the LE serrations approached in this study, there is no material extraction, but instead a deformation to the blade geometry that provides a continuous surface to the blade. These serrations consist in a sinusoidal smooth surface, without edges, in order to be an efficient aerodynamic body. Figure 3 shows a 3D drawing of one of the LE serrated blades, where it is clear the smooth

surface all throughout the blade. The cross section is, also, always the NACA-0018 aerofoil in the serrated part, where the chord results from the sum of two equations: the baseline chord that varies linearly with the span; and the sinusoidal equation characterized by the amplitude $2h$ and the wavelength λ.
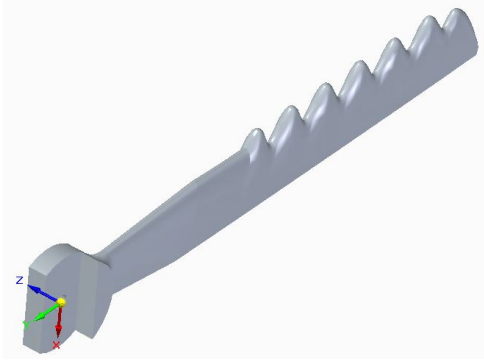

Figure 3: LE serrated blades design.

Following Chong's conclusions and considering Chaitanya's research, the LE serration parameters were defined as the following:

- The amplitude $2h$ varies along the span and equals to 1/3 of the local chord;

- The wavelength λ is constant and equal to $1.5\,cm$.

3.2. Experimental Setup

The experiment is performed inside the Aeroacoustic Wind Tunnel located in the Aerospace Engineering Laboratory of Instituto Superior Técnico. The wind tunnel has a built-in Anechoic Chamber with a designed cut-off frequency of $200Hz$. Figure 4 represents a top view schematic of the chamber. Three microphones are used to collect the noise data, each distancing $2.3m$ from the rotor, with Microphone 0 angled $45°$ from the rotor plane to the wake side, Microphone 1 aligned with the rotor plane and Microphone 2 angled $45°$ from the rotor plane to the suction side.

The noise signal is obtained by the Brüel & Kjær - type 4958 microphones, and then amplified in the PCB Piezotronics 482C15 ICP Sensor Signal Conditioner. Finally, the signal is read and processed using the LabVIEW software from National Instruments. Each test had a collection time of 30 seconds, with a sampling rate of $100000Hz$ and a number of samples of 50000. The LabVIEW program used performed the following acoustic operations:

- A Fast Fourier Transform to convert the results from a time domain to a frequency domain, providing the variation of SPL with frequency;

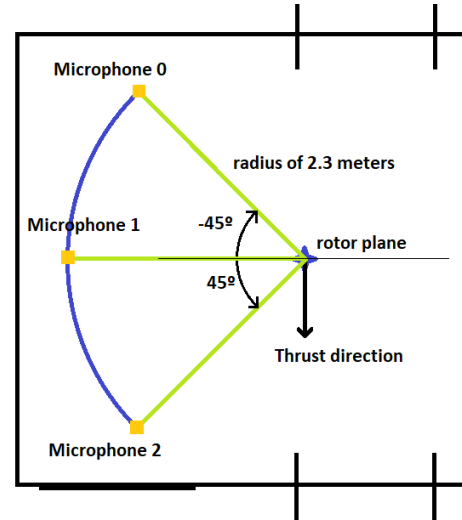- A One-third Octave bands grouping of the SPL;

Figure 4: The microphones positions in the anechoic chamber.

- A calculation of the A-weighted Equivalent Continuous Sound Level (LAeq);

The program also allowed to apply a weighting filter to the noise collected. The A-weighting filter was used in the tests, for it highlights the frequencies to which the human hearing is more sensitive to.

Regarding the measurement of the aerodynamic forces, the workbench mounted by Inês Amado [16] is used, where it was studied the performance of coaxial rotors. In the present study, only one Instrumented Tube is needed, which is represented in Figure 5. A combination of full bending bridges
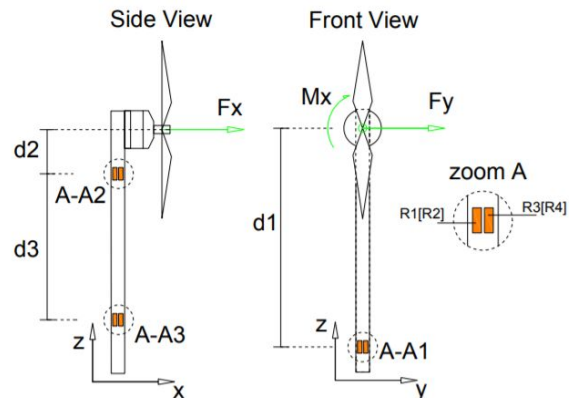

Figure 5: Scheme of the Instrumented Tube. Taken from [16].

is used to measure the thrust F_x, the lateral force F_y and the torque M_x. Knowing the rotation speed Ω in each test, the torque is converted into power P through equation 1.

$$P = M_x \times \Omega \tag{1}$$

4. Results & Discussion
4.1. Noise Assessment

The results were taken for the rotation speeds ranging from 1000 to 4000 Rotations Per Minute

(RPM), with steps of 500 RPM. However, the conclusion is quickly achieved that the speed of 1000 RPM is too low to assess any considerable noise reduction effects, along the frequency spectrum, by the serrated rotors. There is a recurrent trait noticed for every rotor tested, which is that the SPL varying with the frequency read by Mic1 (in the rotor plane) is smaller than the ones read by Mic 0 and Mic2. Figure 6 shows the SPL of the three microphones, measured for the LE40, at 2500 RPM. This phenomenon starts from $350 - 400Hz$ for the shown velocity, which is also common for the other velocities, and it comes to an end at different frequencies, depending on the rotation speed. At 1500 RPM, this difference ends at $5200Hz$; at 2000 RPM, it ends at $14000Hz$; and at 2500 RPM and higher, it occurs until the end of the frequency interval measured. In addition, the difference of the SPL read on the rotor plane, to the other two positions, tends to increase as the rotation speed increases as well.
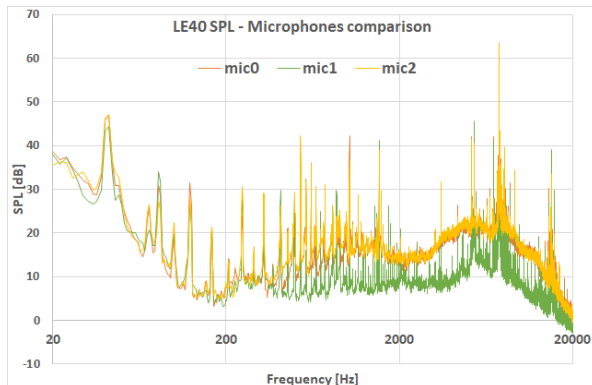

Figure 6: The SPL measured from the three microphones for the LE40, at 2500 RPM.

Overall, the variation of the SPL along the frequency range can be divided into five regions.

First region, at $20 - 200Hz$ **-** The sound waves are reflected in the chamber's walls, ceiling and floor since the cut-off frequency of the anechoic chamber is $200Hz$. In this region, the SPL tends to decrease as the frequency increases, with the exception of three or four peaks. These peaks appear due to the Blade Passing Frequency (BPF), that is the frequency at which the blades rotate. Noise peaks are known to be produced at this frequency and for the multiples of this value, meaning that consecutive peaks are spaced by $BPF = No.\ of\ blades \times RPM/60\ [Hz]$. Accordingly, as the rotation speed is increased, the values of these peaks are higher (naturally because the noise is louder) and the frequency at which they appear increases as well. This effect is noticed in Figure 7 that shows the SPL generated by the TE20 at different rotation speeds. Even so, in these peaks, the noise tends to be reduced by the serrated blades.
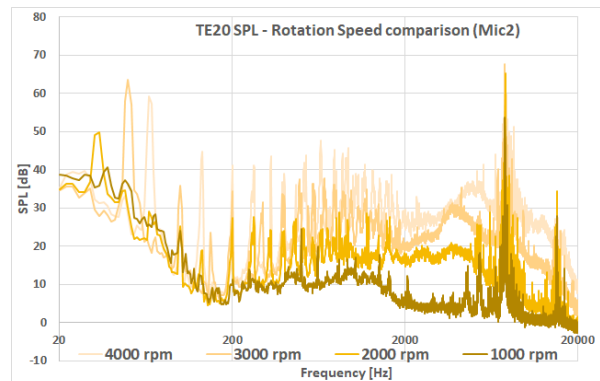

Figure 7: SPL of the TE20 at 1000, 2000, 3000 and 4000 RPM (captured by Mic2).

Second region, at $200 - 1900Hz$ **-** From this region to the following ones the sound is absorbed at the walls, cancelling any sound reflections. Still, similarly to the previous region, there are several peaks in the SPL that, again, are spaced according to the BPF and appear at higher frequencies (and with higher SPL) as the rotation speed increases. This effect is, once more, noticed in Figure 7.

In the present region, the LE rotors reduce the noise comparatively to the baseline, and this noise reduction is greater as the rotation speed is increased. On the other hand, the TE rotors present small increases of the noise, but only for Mic0 and Mic2. For Mic1, the tendency is to reduce the baseline noise just a bit. Figure 8 shows the A-weighted third-octave bands of the serrated rotors in comparison to the baseline at 3000 RPM, for Mic0.

Third region, at $1900 - 7000Hz$ **-** In this region the variation of the SPL is continuous and smooth, in opposition to the several peaks that marked the previous region. Plus, most of this region and part of the previous one correspond to the frequency interval to which the human hearing is most sensitive to, which is from 1000 to $6000Hz$.

The LE rotors produce less noise, in this region, than the baseline for every rotation speed and microphone position tested. For 2500 RPM and higher, the LE20 and the LE60 are the ones that reduce the noise the most, with the LE20 being the best one for 3500 and 4000 RPM. Figure 9 shows the SPL of the LE rotors at 3500 RPM, where the SPL difference between the LE20 and the baseline is always between 5 and $10dB$ throughout this frequency region.

The TE rotors have a distribution of the SPL, relative to the baseline, that varies with the rotation speed. For 1500 RPM, these rotors decrease the noise. However, as the rotation speed is increased (between 2000 and 4000 RPM), the TE rotors produce an ever growing noise increase (in relation to the baseline) in an ever growing frequency interval

(a) LE rotors.

Figure 9: SPL of the LE rotors at 3500 RPM (captured by Mic0).
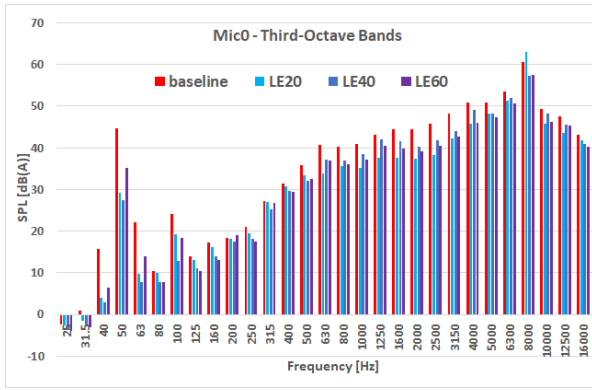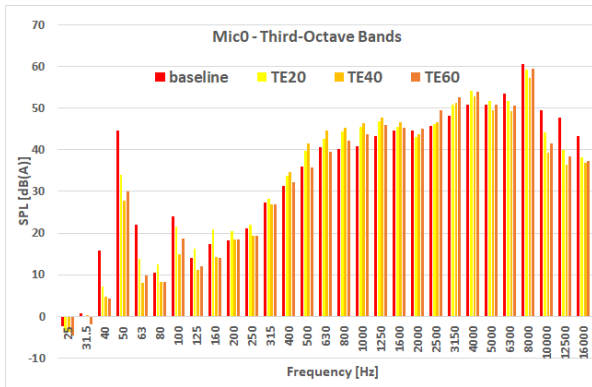
(b) TE rotors.

Figure 8: The third-octave bands distribution at 3000 RPM (captured by Mic0).

(a) 2000 RPM.

(b) 3000 RPM.

Figure 10: SPL of the TE rotors at 2000 and 2500RPM (captured by Mic0).

at the beginning of this frequency region. To simplify this observation, Figure 10 is presented, which shows the SPL variation of the TE rotors for 2000 and 3000 RPM.

Fourth region, at $7000 - 8400Hz$ **-** This is the region which contains the highest noise peak in the SPL distribution, when the A-weighted filter is applied to consider the human hearing sensitivity. Consequently, the value at this peak will be the most important for the calculation of the LAeq for each test. It always appears between 7560 and $7570Hz$ for every rotor and rotation speed, but it is not produced by the blades themselves. This noise peak is mainly generated by the motor when it is being powered to rotate. For most of the frequency spectrum, the motor noise is similar to the background noise, with the exception of some peaks, including the peak addressed for this frequency region. To understand better the influence of the motor noise on the noise collected from each rotor, Figure 11 is presented, which compares the noise produced by the LE20 with the motor noise, at 3500 RPM.

The TE rotors reduce the noise for this region for every speed except for 3500 and 4000 RPM. Without counting with the peak, the LE rotors reduce
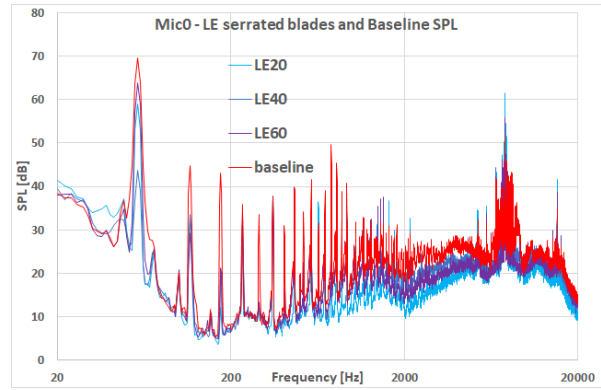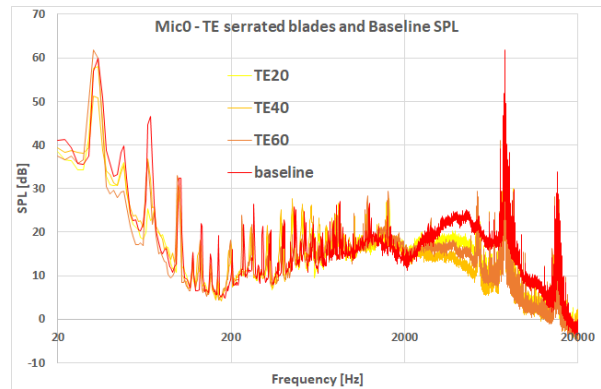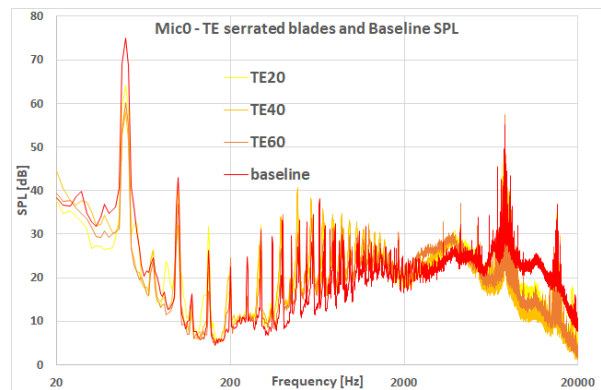
the noise in the whole frequency region, as is seen in Figure 12. But the noise in this region is controlled by the peak value, so the analysis is made towards it. The LE20 presents a noise increase for the peak for every rotation speed, which is unfortunate since this rotor is the one that achieves the greatest noise reduction, relatively to the baseline, for the majority of the frequency spectrum analysed (particularly for the frequencies which the human hearing is more sensitive to). Furthermore, since the LAeq is influenced mainly by the value of this peak, the LAeq of the LE20 is higher than the
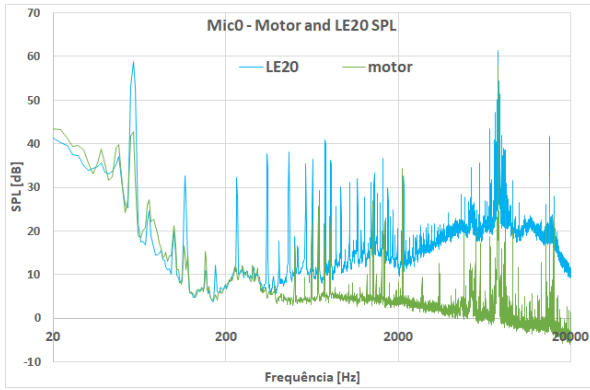
Figure 11: SPL of the motor and of the LE20 rotor, at 3500 RPM (captured by Mic0).
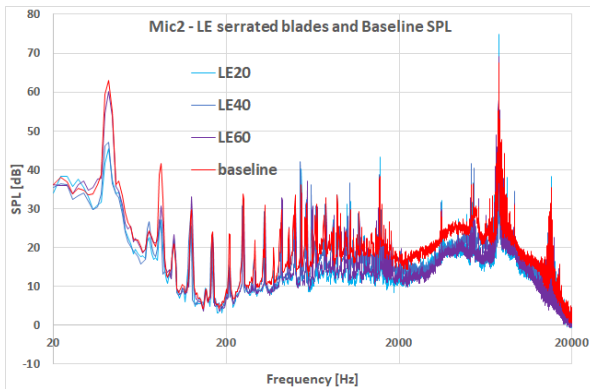

Figure 12: SPL of the LE rotors at 2500 RPM (captured by Mic2).

baseline's for most of the rotation speeds tested. In contrast, the LE40 is the rotor which normally presents the lowest peak value for every speed tested, except for 4000 RPM where it equals the baseline peak's value. Consequently, the LE40 is the rotor that will most likely present the lowest LAeq values. The LE60 increases the peak noise for the higher rotation speeds, but not as much as the LE20. For the rest of the speeds, the LE60 has a similar peak value as the baseline.

Fifth region, at $8400 - 20000Hz$ **-** The noise varies, mostly, continuously and decreasing with the increasing of frequency. There is a noise peak at $15140Hz$, that is exactly the double of the frequency at which appears the big noise peak in the previous region.

In this region, at 2000 RPM and higher, the TE rotors reduce the noise significantly (up to $13dB$) with this reduction being greater as the rotation speed is increased. Figure 13 shows the SPL variation for the TE rotors, where it can be noticed the TE noise reduction for the region in question. It is worth noticing that the blades with the TE serration applied for longer lengths of the span achieve bigger noise reductions. These results were expected since the TE serrations target the TE noise, which is predominant in the higher frequencies of the total
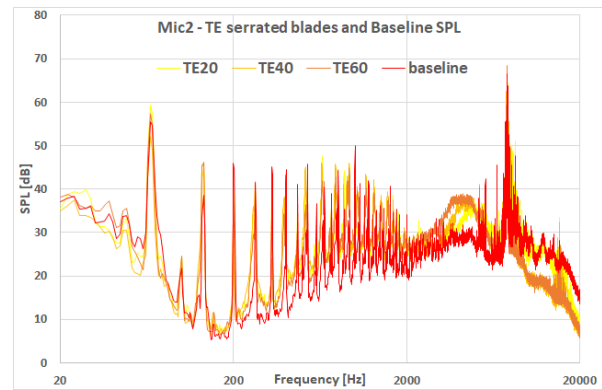
aerodynamic noise.

Figure 13: SPL of the baseline and the TE rotors at 4000 RPM (captured by Mic2).

The LE rotors reduce the noise in this region as well, although clearly not as much as the TE ones, which can be seen in Figure 14, that shows the SPL variation of the LE rotors. This result was also expected because the LE serrations prevent the TE turbulent boundary layer from growing as much as it would if there were no serrations, which leads to weaker noise sources along the TE.
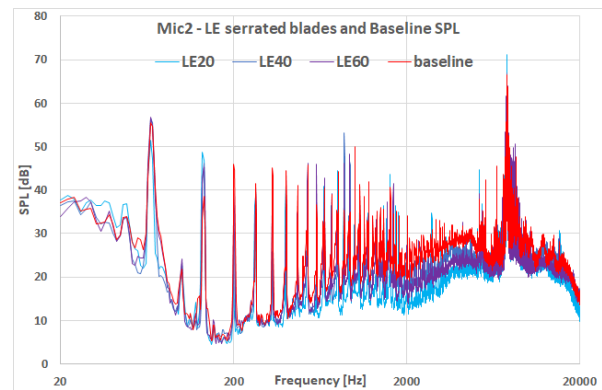

Figure 14: SPL of the baseline and the LE rotors at 4000 RPM (captured by Mic2).

Remembering Soderman's study [11], where it was used a rotor with $1.52m$ of diameter with serrated strips attached to the LE and rotating at a maximum speed of 1440 RPM, it was obtained a maximum noise reduction of $17dB$ in the highest octave band ($16000Hz$). Between 8000 and $16000Hz$, the rotor also achieved noise reductions between 12 and $17dB$, which is considerably bigger than the noise reduction obtained for any of the LE serrated rotors tested. However, between 1000 and $4000Hz$, Soderman's serrated strips reduced the noise between 3 to $6dB$, whereas the present LE serrated blades reached $10dB$ of noise reductions. In addition, Soderman stated to have reached noise reductions of the Overall SPL between 4 to $8dB$, while in the present study the maximum reduction obtained in the LAeq (and in the

total band power) is of $13dB$ with the TE40 at 1500 RPM. Anyway, any comparison of results with the ones obtained by Soderman is qualitatively incorrect because the dimensions of the rotors and the rotation speeds tested are considerably different. Even so, the comparisons made were considered interesting enough to be pointed out.

Having finished the analysis of the SPL per regions, the LAeq can also be regarded. The TE rotors have a reduced LAeq, in comparison to the baseline, for the rotation speeds between 1500 and 3000 RPM. However, for the highest tested speeds, the TE rotors have a bigger LAeq than the baseline. In the case of the LE20, it has, mostly, a bigger LAeq than the baseline due to the SPL peak at $7570Hz$. The LE40 has, in general, a lower LAeq than any other rotor. The LE60 has a lower LAeq than the baseline in most cases, but it is not as reduced as the one produced by the LE40.

4.2. Aerodynamic Assessment

In the figures that will be presented along this section, one notices that every rotor has a very poor performance for the two lowest rotation speeds, meaning that any typical rotor of similar dimensions to the ones presented in this thesis will unlikely operate at these lowest rotation speeds. Therefore, the aerodynamic assessment presented will, to some extent, overlook the results obtained for these rotation speeds.

Figure 15 shows the percentage of the thrust coefficient C_T of each serrated rotor in relation to the C_T of the baseline. The worst rotor in terms of thrust generated is the TE40, for rotation speeds 1500 RPM and higher. The TE20 has a percentage of thrust between 50% and 75% for the lowest rotation speeds, but then this value remains steady around 80% for speeds between 2000 and 4000 RPM. The TE60 shows a percentage of C_T constantly increasing with the rotation speed and reaching a value higher than the TE20 for speeds equal and higher than 3000 RPM, which is quite surprising since the blades of this rotor are the ones that have the TE serration applied for the longer span of the blade. Noting also that comparing the TE40 with the TE60 (with a difference of 20% of the span of the blades serrated), the latter has always a percentage of C_T higher by around 10% for rotation speeds of 2000 RPM and higher. Lee *et al.* [8] presented a percentage of thrust loss around 15% for TE serrated blades over 25% of the span, tested for rotation speeds between 1500 and 3000 RPM. For blades serrated over 50% of the span, the thrust loss decreased between 27% and 22% as the rotation speed increased, similar to the results here presented.

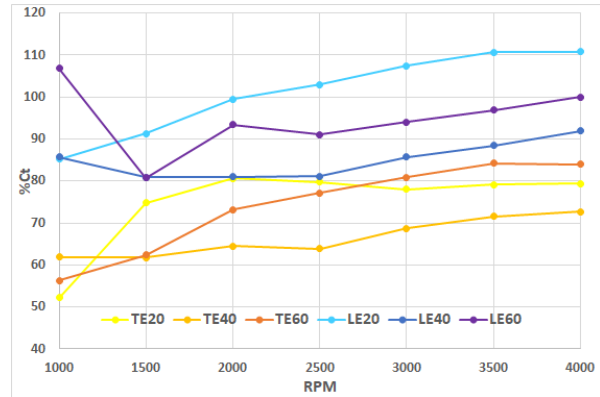The LE rotors experienced smooth modifications

Figure 15: Percentage of C_T in relation to the baseline.

to the LE. Consequently, their thrust is closer to the one generated by the baseline in comparison to the TE rotors. In general, and evaluating only between 2000 and 4000 RPM, the percentage of thrust relative to the baseline increases as the rotation speed increases. The LE40 is the rotor which generates the lowest thrust, of the three LE rotors, with a percentage of C_T between 81% and 91%. The LE60 generates between 91% and 100% of the baseline's thrust, whereas the LE20 surpasses the baseline with values between 100% and 111%. Chong *et al.* [13] studied wings with sinusoidal LE and concluded that higher values of the serration amplitude led to higher losses to the C_L and C_{L_α} coefficients. However, for small serration amplitudes and large serration wavelengths, the C_L showed almost neglectable losses, but the stall angle would become considerably higher, which could be considered as an improvement to the overall aerodynamic qualities of the wing.

Figure 16 presents the percentage of the power coefficient C_P in relation to the baseline. Every rotor has a higher power than the baseline, except the LE40. This rotor has lower power for rotation
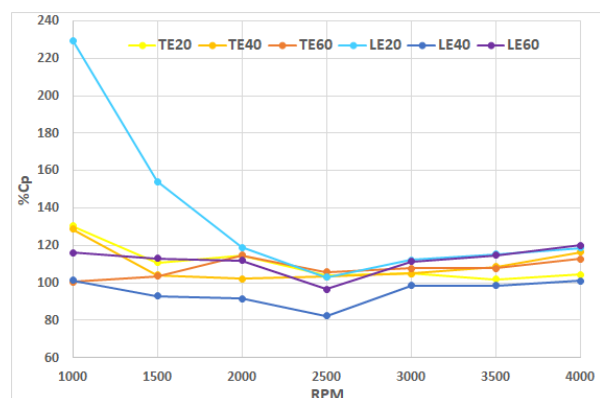

Figure 16: Percentage of C_P in relation to the baseline.

speeds between 1000 and 3000 RPM, reaching a minimum value of percentage of C_P of 82% at 2500 RPM, and a value close to 100% for at 3000, 3500

and 4000 RPM. The other five serrated rotors have a percentage of C_P between 100% and 120% for the most relevant rotation speeds. The three LE rotors present all a minimum for 2500 RPM, while the three TE rotors present a very small variation of the percentage of C_P with the rotation speed. Curiously, although the LE40 is the rotor with the lowest percentage of C_P for rotation speeds between 3000 and 4000 RPM, the LE20 and LE60 have the higher values. For the mentioned speeds, the TE20 presents almost the same C_P as the baseline.

Figure 17 shows the Figure of Merit (FM) obtained from the tests, and there are four remarks to mention. First, the FM tends to increase as the rotation speed increases. Second, the TE rotors consistently present the lowest values, with TE40 being the worst with a maximum FM of 0.117 and both TE20 an TE60 with maximums of 0.15. Third, taking only into account the speeds equal and higher than 2000 RPM, the LE40 and the LE60 have an almost identical variation, which are clearly more efficient than the TE rotors but still worse than the baseline. Fourth, the LE20 has relatively low values of FM at lower rotation speeds. However, it reaches similar values as the baseline between 2500 and 4000 RPM. The same LE20 rotor generated a higher thrust than the baseline, but also a higher power. Therefore, concerning the aerodynamic performance, the LE20 is, in the bare minimum, as interesting as the baseline.
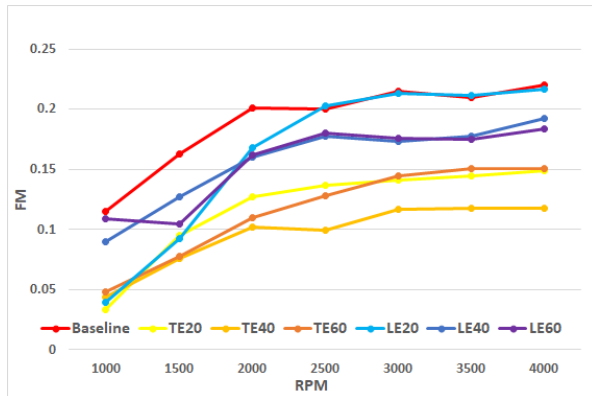

Figure 17: The FM obtained for all the rotors.

The different serrated blades have a different surface area from the baseline, due to the serrations applied. So, in order to evaluate the thrust generated weighted by the different surface areas, the term C_T/σ was calculated, where $\sigma = 2 \times A_p/A$ is the rotor solidity, A the rotor area and A_p is the blade planform area. Figure 18 shows the variation of the FM and the C_T/σ for the tested rotors and rotation speeds. Once again, the LE20 shows an aerodynamic performance quite interesting for the higher rotation speeds. On the other hand, the TE

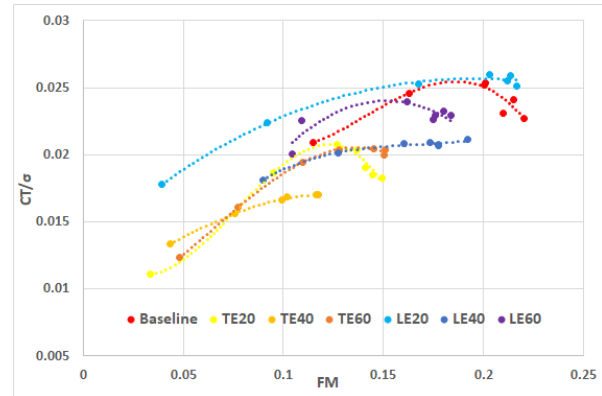serrations degrade considerably the aerodynamic performance of the blades.

Figure 18: Comparison of the C_T/σ versus the FM.

Considering the satisfactory characteristics of the LE20, the LE40 has a far worse performance in terms of both C_T/σ and FM. However, with 60% of the LE serrated (LE60), there is an improvement of the aerodynamic characteristics, which leads to the conclusion that there are, at least, two optimum configurations concerning this kind of LE modifications: one close to the 20% of the serrated LE, and the other close to the 60%. This conclusion does not solely apply to sinusoidal LE, for there might be other types of curved and smooth geometries that, while implemented to the LE, might provide results as interesting as these ones.

5. Conclusions

The noise generated by an operating rotor is not directionally uniform, for it is clear that the noise in the rotor plane is lower than at $45°$ to either the suction or to the wake sides. Even so, for any of the directions, the serrated rotors can achieve noise reductions, in comparison to the baseline, for at least some intervals of the frequency spectrum. However, the noise reductions are highly dependant on the rotation speed, and the same rotor can reduce the noise for some speeds and increase for others.

The TE serrated blades are effective in reducing the high frequency noise for any rotation speed, but the LAeq measured increases significantly for the higher tested speeds. So, acoustically, these blades are only worth using for the lower-to-moderate speeds. However, considering the aerodynamic performance, the TE serrated rotors are never worth being used for any rotation speed because they clearly degrade the aerodynamic qualities. Comparing to the baseline, these rotors generate considerably less thrust and require more power, which leads to a very low efficiency. Overall, and comparing with the LE serrated rotors, the TE serrations do not seem a viable feature to implement in real rotors of small UAVs.

The LE serrated blades proved to reduce the noise in the mid-range frequencies, which correspond to the noise frequencies that the human hearing is most sensitive to. In addition, these blades also achieved small noise reductions for the high frequency noise. However, they presented, as well, increases in the measured LAeq for some rotation speeds, specially the LE20 rotor. This rotor was the one to obtain the best reductions in the SPL, in comparison to the baseline, but it also obtained, consistently, the bigger LAeq values due to increasing the noise in the frequency at which the motor noise was higher. In opposition, the LE40 rotor reduced the LAeq for every rotation speed, even though it did not reduce the mid-frequencies SPL as much as the LE20. Furthermore, regarding the aerodynamic performance, the LE serrated rotors presented quite interesting results, with the LE20 over-performing the baseline for the mid-to-high rotation speeds in terms of thrust and of FM. The other two LE serrated rotors did not perform so well, but still they had higher thrust and efficiency than the TE serrated rotors. All in all, the LE serrations are an interesting option to implement on rotating blades, for both acoustical and aerodynamic reasons, and, in the present thesis, one could say that the best compromise is found either in the LE20 or in the LE60 rotors.

This thesis focused, partly, on sinusoidal LE modifications, but hopefully it demonstrates that the use of other types of curved and smooth LE modifications on rotating blades are worth studying because they could be beneficial for both aerodynamic and acoustic purposes, as it was found to be during this study.

References

[1] R. K. Amiet. Acoustic radiation from an airfoil in a turbulent stream. *Journal of Sound and Vibration*, 41(4):407–420, 1975.

[2] R. K. Amiet. Noise due to turbulent flow past a trailing edge. *Journal of Sound and Vibration*, 47(3):387–393, 1976.

[3] M. S. Howe. Aerodynamic noise of a serrated trailing edge. *Journal of Fluids and Structures*, 5(1):33–45, 1991.

[4] M. S. Howe. Noise produced by a sawtooth trailing edge. *Journal of the Acoustical Society of America*, 90(1):482–487, 1991.

[5] S. Sinayoko, M. Azarpeyvand, and B. Lyu. Trailing edge noise prediction for rotating serrated blades. *20th AIAA/CEAS Aeroacoustics Conference*, pages 1–20, June 2014.

[6] Benshuai Lyu, Mahdi Azarpeyvand, and Samuel Sinayoko. Noise prediction for serrated leading-edges. *22nd AIAA/CEAS Aeroacoustics Conference, 2016*, 2016.

[7] Mathieu Gruber, Phillip F. Joseph, and Tze Pei Chong. On the mechanisms of serrated airfoil trailing edge noise reduction. *17th AIAA/CEAS Aeroacoustics Conference 2011 (32nd AIAA Aeroacoustics Conference)*, pages 5–8, June 2011.

[8] Hsiao Mun Lee, Zhenbo Lu, Kian Meng Lim, Jinlong Xie, and Heow Pueh Lee. Quieter propeller with serrated trailing edge. *Applied Acoustics*, 146:227–236, 2019.

[9] Alan S. Hersh and Richard E. Hayden. Aerodynamic sound radiation from lifting surfaces with and without leading-edge serrations. *Report CR-114370, NASA*, September 1972.

[10] Paul T. Soderman. Aerodynamic effects of leading-edge serrations on a two-dimensional airfoil. *NASA Technical Memorandum TM X-2643*, September 1972.

[11] P. T. Soderman. Leading edge serrations which reduce the noise of low-speed rotors. *NASA Technical Note TN D-7371*, August 1973.

[12] Alan S. Hersh, Paul T. Soderman, and Richard E. Hayden. Investigation of acoustic effects of leading-edge serrations on airfoils. *Journal of Aircraft*, 11(4):197–202, 1974.

[13] Tze Pei Chong, Alexandros Vathylakis, Archie Mcewen, Foster Kemsley, Chioma Muhammad, and Saarim Siddiqi. Aeroacoustic and aerodynamic performances of an aerofoil subjected to sinusoidal leading edges. *21st AIAA/CEAS Aeroacoustics Conference*, 2015.

[14] P. Chaitanya, S. Narayanan, P. Joseph, C. Vanderwel, J. Turner, J. W. Kim, and B. Ganapathisubramani. Broadband noise reduction through leading edge serrations on realistic aerofoils. *21st AIAA/CEAS Aeroacoustics Conference*, pages 1–29, June 2016.

[15] Michel Roger, Christophe Schram, and Leandro de Santana. Reduction of airfoil turbulence-impingement noise by means of leading-edge serrations and/or porous materials. *19th AIAA/CEAS Aeroacoustics Conference*, page 105, 2013.

[16] Inês Silva Amado. Experimental Comparison of Planar and Coaxial Rotor Configurations in Multi-rotors. *Master Thesis, Instituto Superior Técnico*, September 2017.